Int J. Multiphase Flow Vol. 18, No 1, pp. 21–33, 1992
Printed in Great Britain. All rights reserved

0301-9322/92 $5.00 + 0.00
Copyright © 1992 Pergamon Press plc

PARTICLE VELOCITY CHARACTERISTICS OF DILUTE TO MODERATELY DENSE SUSPENSION FLOWS IN STIRRED REACTORS

J. M. NOURI and J. H. WHITELAW

Mechanical Engineering Department, Fluids Section, Imperial College of Science, Technology and Medicine, Exhibition Road, London SW7 2BX, England

(Received 15 May 1990; in revised form 15 July 1991)

Abstract—Measurements of particle mean and r.m.s. velocity were obtained by laser–Doppler velocimetry in solid–liquid turbulent flows in fully baffled stirred reactors driven by Rushton-type impellers of different sizes at rotational speeds of 150, 300 and 313 rpm. The effects of particle size, density and volumetric concentration were investigated. The maximum particle concentration at which the solid-phase velocity measurements could be made was improved from 0.02 to 2.5% when the refractive index of the continuous-phase was matched to that of the dispersed particles. The results showed a steep particle concentration gradient in the vertical direction below the impeller and a mild one above the impeller, that the particles lagged or led the bulk fluid when the flow direction was upwards and downwards, respectively, and that the particle turbulence levels were in general lower than those of the single-phase flow levels, especially in the impeller stream and wall jet regions. Particle velocities decreased with an increase in particle concentration, while the particle turbulence levels remained the same. The apparent relative velocity of glass particles was higher than that of Diakon by up to 2.5 times and the effect of the particle size, at least for the sizes used in the experiment, was negligible.

Key Words: stirred reactors, particle suspensions, velocities

1. INTRODUCTION

Stirred reactors are widely used in the chemical and food processing industries. The mixing process is important in the design of the stirred reactors (Oldshue 1983) and requires an understanding of fluid mechanic characteristics since it is accomplished, in turbulent mixing, by bulk flow, eddy diffusion and molecular diffusion (Uhl & Gray 1966). The flow in stirred reactors is usually turbulent, recirculating and three-dimensional and, when multiphase mixing is involved, the complexity increases. The present work quantifies the flow patterns of the dispersed phase in the stirred vessels and the effects of particle size, density and concentration by measuring the mean and r.m.s. of the three components of particle velocity. Single-phase turbulent flow characteristics in stirred reactors are not considered here since they have been investigated by a number of researchers, including Yianneskis *et al.* (1987), Nouri (1988) and Nouri & Whitelaw (1990) who used laser–Doppler velocimetry and showed that flow generated by a Rushton-type impeller is of a double-vortex structure, with the direction of rotation imposed by the radial jet stream which emanates from the tip of the impeller.

In two phase-flow, there is little information on the velocity of either phase in stirred vessels. Measurements of solid or droplet suspensions in fluids have been investigated mainly in pipe and jet flows to determine the effects of particle inertia, crossing-trajectories, particle–particle and particle–fluid interactions, turbulence and drag, and the results have been reviewed, for example, by Nouri (1988). Laser–Doppler velocimetry has been employed for the measurement of the velocity of each phase as, for example, by Einav & Lee (1974), Lee & Durst (1982) and Modarress *et al.* (1982, 1983). The use of amplitude discrimination for measurements of the dispersed phase is satisfactory but it is unable to distinguish perfectly between Doppler signals of large and small particles (Durst 1982). An alternative method was suggested by Durst & Zare (1975) and involves the phase shift between Doppler signals at different angles of observation and has been used, for example, by Bachalo & Houser (1984), Saffman *et al.* (1986) and Hardalupas (1986).

In two-phase flows, blockage of the transmitting and scattered light by the dispersed phase has limited measurements to dilute flow suspensions of particle volumetric concentration of $< 1.5\%$

(e.g. Lee & Durst 1982; Nouri *et al.* 1984). To measure in dense solid–liquid flow suspensions, Nouri *et al.* (1988) developed a technique in which the refractive index of a mixture of tetraline and the oil of turpentine was matched to that of Diakon particles, and showed (Nouri *et al.* 1987; Liu *et al.* 1990) that results could be obtained with volume fractions of 14 and 11.3% in depth of flow fields of 25.4 and 38.1 mm, respectively.

Particle-to-particle interactions are expected to be significant for volumetric concentrations $> 0.3\%$ (Lumley 1978), the pressure drop and friction factor increase with concentration (Cox & Mason 1971; Tsuji & Morikawa 1982) and the suspension would behave like a non-Newtonian fluid at very high particle concentration (Soo 1967). The effect of particle crossing-trajectories and inertia on the dispersion of the particles in turbulent flow was investigated by Wells & Stock (1983), who concluded that crossing-trajectories decreased the dispersion of the particles when the particle free-fall velocity was greater than the fluid r.m.s. velocity, and that of inertia reduced the r.m.s. velocity. In a recirculating flow, Nouri *et al.* (1987) showed that the length of the recirculation zone of the dispersed-phase flow, behind an axisymmetric disc baffle, was shorter than that of single-phase flow by 11 and 24% for concentrations of 4 and 8%, respectively. Particle velocities in a swirling, confined flow were reported by Liu *et al.* (1990), who showed that when the particles were suspended in the annulus, the induced swirl centrifuged the beads to large radii causing local regions of high concentration and turbulence suppression.

In the present investigation, a refractive index matching technique was used in conjunction with laser–Doppler velocimetry to measure single- and solid-phase velocities in stirred vessels. The flow configuration and experimental techniques are described in the following section, the results are presented and discussed in section 3, and the paper ends with a summary of findings.

2. FLOW CONFIGURATION AND INSTRUMENTATION

The mixing vessel and impellers are shown in figure 1. The mixing was constructed from an acrylic (Perspex) cylinder of inside diameter $T = 294$ mm. Four baffles of width $T/10$ were located along the vessel periphery and 6-bladed impellers were used. The impeller diameter, D, blade length, L, and blade height, h, were in the ratio $D{:}L{:}h = 1{:}4{:}5$, an arrangement commonly used in real mixing vessels. The thickness of the blades, disc and baffles was 3 mm and the shaft diameter was 12.7 mm. The impellers, the shaft and baffles were all made of clear Perspex. The vessel was placed inside a rectangular box, also made of Perspex, and the intervening spaced filled with the same fluid as inside the vessel so as to reduce problems associated with refraction by the curved surface. The mixing vessel was mounted on a traversing bench which allowed translation in three directions.

The working fluid was water and a mixture of 32.0% by vol of tetraline and oil of turpentine. The former allowed measurements with dilute suspensions, while the latter was used to improve light-beam penetration in denser suspension flows. In the case of the mixture flow, the temperature of the fluid was controlled to 28.5 ± 0.02°C so that its refractive index was 1.488, identical to that of the Perspex. Table 1 summarizes the flow conditions considered here.

The impeller tip velocity, Reynolds number and power number in table 1 were calculated from the expressions, $V_t = \pi ND$, $\mathrm{Re} = ND^2/\nu$ and $N_p = P/\rho N^3 D^5$, where P is the power input into the vessel obtained from the measurements of the induced torque and ν and ρ are fluid viscosity and density, respectively. The flow response time was defined as the ratio of impeller width (h) to the impeller tip velocity.

Diakon and lead-glass particles of different sizes were used as the dispersed phase in water flow suspension and Diakon in the mixture flow. The maximum particle volumetric concentration was 0.02% when the particles were suspended in water, and this was increased to 2.5% with refractive index matching. Particle inertia effects may be characterized by the response time, given as

$$\tau_p = (d_p)^2\{[2\rho_p/(\rho - 1)]/(36\,\nu)]\}, \qquad [1]$$

where d_p and ρ_p are particle diameter and density, respectively, and, since the fluid density is much greater than unity, this equation can be written as

$$\tau_p = (d_p)^2\rho_p/(18\,\mu), \qquad [2]$$

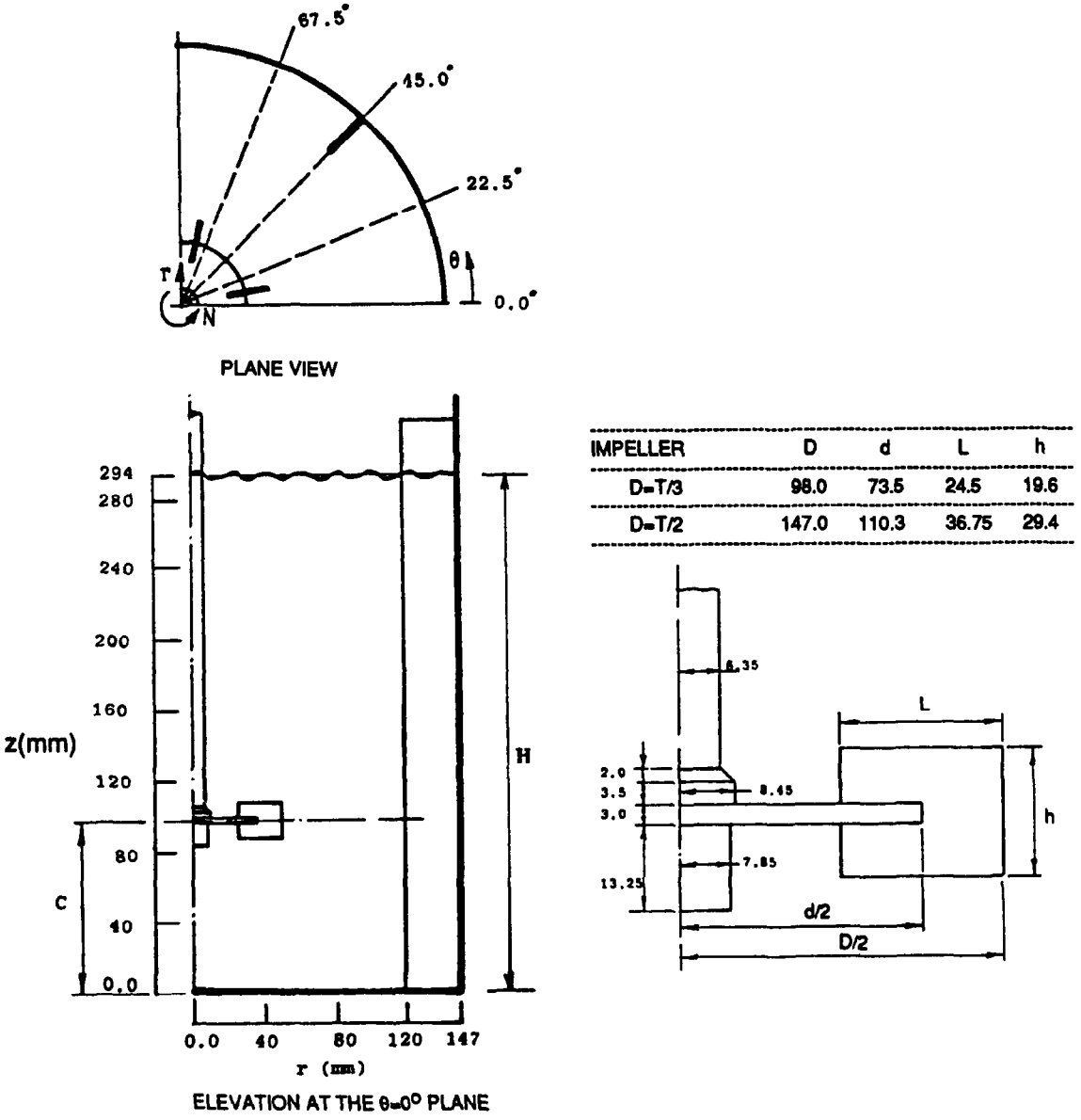

Figure 1. Flow configuration, dimensions and coordinate system (all dimensions in mm).

where μ is the dynamic viscosity of the fluid. The terminal velocity of the particle in the Stokes law region and in the turbulent region, based on drag and gravity considerations, are obtained from

$$V_{Gs} = (d_p)^2(\rho_p - \rho)g/(18\,\mu) \quad [3]$$

and

$$V_{Gt} = \{\sqrt{[4d_p(\rho_p - \rho)g/(3\rho C_d)]}\}, \quad [4]$$

Table 1. Flow condition

	Water flow		Mixture flow
Impeller diameter, D	$T/2$	$T/3$	$T/3$
Impeller clearance, C	$T/4$	$T/3$	$T/4$
Impeller speed, N (rpm)	150.0	300 0	313.0
Impeller tip speed, V_t (m/s)	1.115	1.54	1.6
Reynolds number, Re ($\times 10^3$)	54.0	48 0	32.5
Power number, N_p	5.0	4.7	4.4
Flow response time, τ_f (ms)	25.0	13.0	12.0

Table 2. Fluid and particle properties

Properties	(I) Water flow at room temperature (20°C) Water	Diakon		Lead-glass	
Density (kg/m^3)	998	1180		2950	
Density ratio, ρ_p/ρ		1.18		2.95	
Kinematic viscosity, ν ($\times 10^{-6}$m/s^2)	1.02	—		—	
Refractive index at $\lambda = 589.6$nm	1.334	1.49		1.60	
Particle size range (μm)		180–450 & 600–850		100–400 & 200–500	
Particle mean diameter, d_p (μm)	—	272.0	725.0	232.0	367.0
Particle terminal velocity, V_{gs} (mm/s)	—	7.2	51.7	57.5	144.0
Particle terminal velocity, V_{Gt} (mm/s)	—	38.0	62.0	116.0	146.0
Particle Reynolds number, Re_p	—	10.0	45.0	27.0	54.0
Particle response time, τ_p (ms)		5.0	34.0	9.0	22.0

Properties	(II) Mixture flow at 28.5°C Mixture	Diakon
Volumetric percentage of tetraline, C_m	32.6	—
Density, kg/m^3		894 1180
Density ratio, ρ_p/ρ	—	1.32
Kinematic viscosity, ν ($\times 10^{-6}$m/s^2)	1.54	—
Refractive index at $\lambda = 589.6$nm	1.4884	1.4884
Particle size range (μm)	—	590–730
Particle mean diameter, d_p (μm)	—	665.0
Particle terminal velocity, V_{Gs} (mm/s)	—	50.0
Particle terminal velocity, V_{Gt} (mm/s)	—	76.0
Particle Reynolds number, Re_p		50.0
Particle response time, τ_p (ms)	—	21.0

where g is the gravitational acceleration and C_d is the drag coefficient, taken as 0.44. The effect of particles on fluid turbulence can be characterized by the particle Reynolds number, as suggested by Hetsroni (1989), based on the particle terminal velocity in turbulent flow, fluid viscosity and particle mean diameter as

$$Re_p = V_{Gt}\, d_p/\nu. \qquad [5]$$

The properties of the fluids and of the particles are given in table 2, for water and mixture flows, respectively. The values of Re_p are small ($Re_p < 110$) and this suggests that the particle will tend to suppress fluid turbulence.

Diakon particles of diameters up to 700 μm remained suspended in the flow with the standard impeller geometry ($D = C = T/3$) at the maximum operational speed ($N = 300$ rpm), but were observed to settle on the bottom of the vessel for larger diameters. The maximum operational speed is defined as the speed above which air bubbles were entrained into the flow system from the free surface. With glass particles, about 50% of 232 μm dia particles were suspended in the flow and the rest deposited on the vessel bottom; with 367 μm dia glass particles only a small number remained suspended. By changing the geometry to $D = T/3$ and $C = T/4$ for Diakon and to $D = T/2$ and $C = T/4$ for lead-glass, more vigorous mixing was achieved near the bottom of the vessel and a larger proportion of particles remained in suspension; the maximum impeller speed in the former geometry was 313 rpm, with which more than 95% of particles were suspended. The impeller speed for the second geometry had to be reduced to 150 rpm to prevent entrainment of air bubbles and about 90% of the 232 μm dia and at least 50% of the 367 μm dia of glass particles were suspended. A relative concentration gradient along the height of the vessel was quantified for the Diakon particles and the result is presented in subsection 3.2.

Table 3. Two-phase flow configurations investigated

Particle material	Liquid	d_p (μm)	D	C	N (rpm)	Temperature (°C)	C_v (%)	Stokes No. (τ_f/τ_p)
Diakon	Water	272.0	$T/3$	$T/3$	300.0	20 ± 1.0	0.02	2.60
Diakon	Water	725.0	$T/3$	$T/3$	300.0	20 ± 1.0	0.02	0.39
Lead-glass	Water	232 0	$T/3$	$T/3$	300.0	20 ± 1.0	0.02	1.45
Lead-glass	Water	232 0	$T/2$	$T/4$	300.0	20 ± 1.0	0 02	2.78
Lead-glass	Water	367.0	$T/2$	$T/4$	150.0	20 ± 1.0	0.02	1.14
Diakon	Mixture	665.0	$T/3$	$T/4$	313.0	28.5 ± 0.02	0 to 0.25	1.45

Table 4. Characteristics of the optical arrangement

Half-angle of the beam interaction (deg)	8.9
Fringe spacing (μm)	2.045
No. of fringes without frequency shift	61
Diameter of the control volume at $1/e^2$ intensity (μm)	125.0
Diameter of the control volume at $1/e^2$ intensity (μm)	1063.0
Maximum frequency shift (MHz)	± 1.75
Frequency to velocity conversion (ms^{-1}/MHz)	2.045

The two-phase flow geometries considered here are summarized in table 3, the measurements with the first five cases were made in water at low volumetric concentration ($C_v = 0.02\%$) and those with the last case in a mixture of tetraline and turpentine with particle concentrations of up to 2.5%. It is anticipated that the results of the first five cases are unaffected by the variation in concentration, as the particle separations are large and particle-to-particle interaction should be negligible. These effects are expected to be more significant with a particle concentration of 2.5%.

The Stokes number in table 3 is defined as the ratio of the single-phase flow response time, based on blade width and impeller tip speed, to the particle response time and is a measure of particle response to the flow. The values in table 3 suggest that the particles will follow the fluid motion, except for the 665 and 725 μm Diakon particles.

The impellers were driven by a d.c. motor (Bodine Electric Co. model 179) and the maximum variation in impeller speed did not exceed $\pm 0.25\%$ of the impeller tip velocity. The impeller shaft gave rise to precession of up to 1.0 mm in the vessel but this did not affect the deductions of the following sections. An optical encoder was fitted to the shaft and provided a train of 2000 pulses/revolution which allowed the impeller rotational speed to be measured and continuously monitored.

The laser–Doppler velocimeter was identical to that described by Nouri (1988) and comprised a 5 mV helium–neon laser, diffraction-grating unit to divide the light beam and provide frequency shift, a focusing lens to form the control volume in the test section, a lens located on the axis to collect forward-scattered light, a pin hole and photomultipler. The principal characteristics of the optical system are given in table 4. The signal from the photomultipler was processed by a frequency counter interfaced to a microprocessor and led to time-averaged (over 360°) values of mean and r.m.s. velocities. Measurements of the mean and r.m.s. velocity components of single-phase were measured first and then, by reducing the photomultiplier sensitivity and closing partially the adjustable aperture placed in front of the photomultiplier, all the Doppler signals corresponding to the fluid were eliminated. The beads were then inserted and their mean and r.m.s. velocity components were measured. The uncertainties associated in mean and r.m.s. values are $< 1\%$ and $< 3\%$ of the local values, respectively, increasing to 2.5 and 5% in the regions of steep and non-linear velocity gradient.

Due to the presence of gas-inclusions inside the Diakon particles, measurements of liquid-phase velocity in the presence of the particles could not be made unambiguously. These inclusions also affected the transparency of the flow field so that the solid-phase measurements were limited to a maximum particle concentration of 2.5%. Since the liquid-phase velocities cannot be measured, then it is useful to define an apparent relative velocity, for comparison purposes, as the mean component particle velocities minus the corresponding fluid velocity in the absence of the particles denoted by subscript s; i.e. U_s, V_s and W_s are the apparent relative velocity in the axial, radial and tangential direction, respectively.

3. RESULTS AND DISCUSSION

A measure of the accuracy of the measurements may be deduced from table 5 which presents values of axial mass flow, Q_{in}, into the impeller from above and below and the radial discharge along the tip of the impeller, Q_r. These results were obtained from integration of axial and radial profiles of mean velocity in vertical (r–z) planes. The differences between Q_r and Q_{in} are $< 5\%$ and, considering the interpolation uncertainties, the agreement is excellent.

The solid particle mean and r.m.s. velocity results for two-phase flows in a stirred vessel are presented in this section together with the corresponding single-phase results for comparison. All

Table 5. Mass balance around the impeller in the r–z plane

Impeller diameter, D	Impeller clearance, C	Impeller speed, N(rpm)	Radial discharge outflow at the impeller tip, Q_r (kg/s)	Total mass inflow from above and below the impeller, Q_{in} (kg/s)	Q_r/Q_{in}
$T/3$	$T/3$	300	4.05	3.88	1.044
$T/3$	$T/4$	313	4.25	4.31	0.98
$T/2$	$T/4$	150	7.30	7.66	0.95

the velocities have been normalized with the impeller tip speed and the radial distance with the impeller radius. The results are presented under two headings: particle motion in dilute and moderately dense suspensions, respectively.

3.1. Particle motion in a dilute suspension

The mean and r.m.s. velocities of the first three particles in table 3 are presented in figures 2 and 3 together with corresponding single-phase flow results. The profiles of figure 2 show that the radial particle velocities differ from those of the single-phase flow near the plane of the impeller disc where the 725 μm dia Diakon particles and 232 μm dia glass particles lag behind the fluid, with an apparent relative velocity, V_s, of about 96 and 200 mm/s or 0.06 and 0.13 V_t, respectively; the apparent relative velocity of heavier particles (lead-glass) is twice that of the lighter particles (Diakon). This lag around the peak of the stream jet is in agreement with the results presented by Nouri *et al.* (1984, 1987) in flows around axisymmetric baffles in horizontal and vertical pipes and contrasts

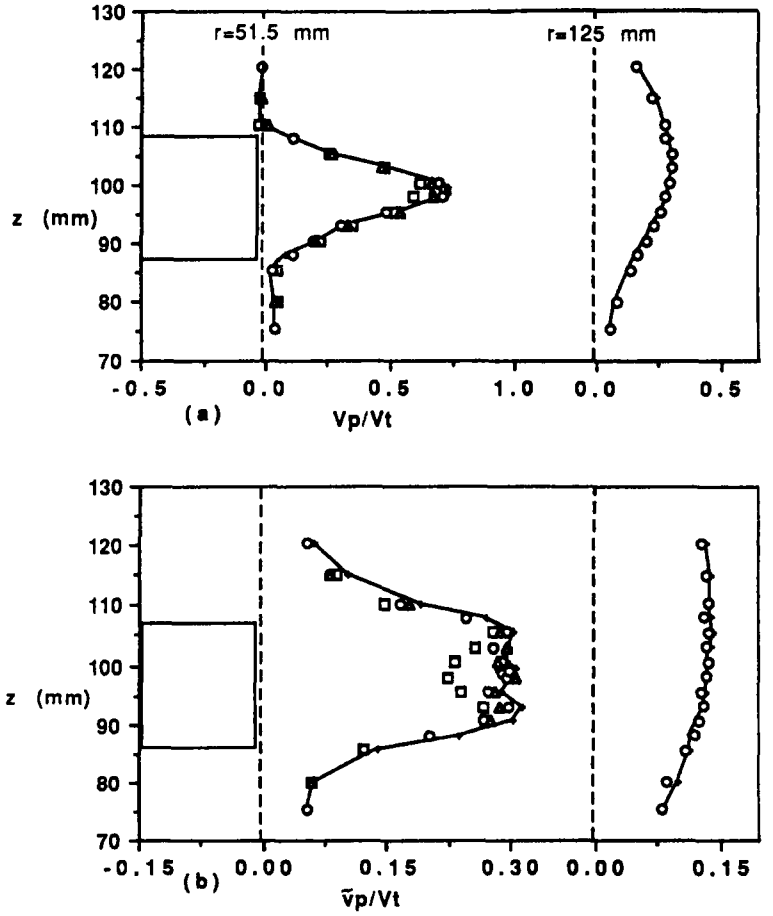

Figure 2. Particle radial velocities in the impeller stream for $D = C = T/3$, $N = 300$ rpm and $\theta = 0$: (a) mean; (b) r.m.s. —+—, Single phase; ○, Diakon 272 μm; △, Diakon 725 μm; □, glass 232.5 μm; ◇, glass 376 5 μm

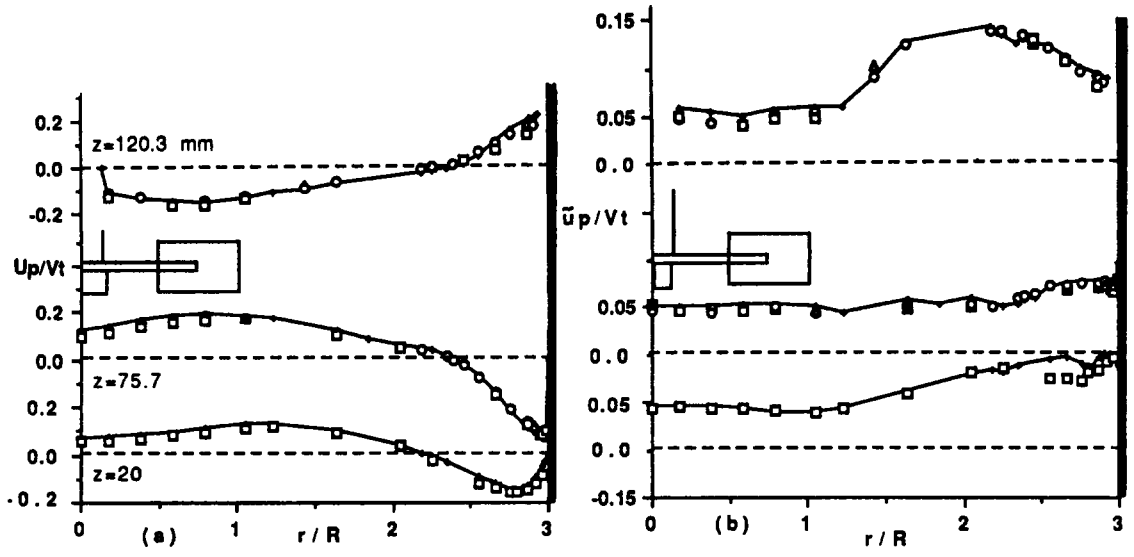

Figure 3. Particle axial velocities above and below the impeller for $D = C = T/3$, $N = 300$ rpm and $\theta = 0°$: (a) mean; (b) r.m.s. Symbols as in figure 2.

with calculated values of relative velocity, of about 38 and 116 mm/s for Diakon and glass particles, respectively. The 272 μm dia Diakon particles appear to follow the flow with negligible slip.

The particle turbulence levels in the impeller stream are less than those with single-phase flow especially at the tip of the impeller ($r = 51.5$ mm) and along the impeller width, with a maximum reduction of 25% at the centre of the blade for the heavier particles. The reduction of turbulence levels for the Diakon particles in the same region is about 13% and at $r = 125$ mm the difference in Diakon particle and single-phase turbulence levels and at $r = 125$ mm the difference in Diakon particle and single-phase turbulence levels is small and within experimental error.

In the bulk of the flow, the axial particle velocity profiles, figure 3, suggest small apparent relative velocities and that the particles lag behind the fluid in upflow due to gravity, as in the flow region in the wall jet above the impeller and around the axis below the impeller where the flow is entrained into the impeller, and lead the fluid in downflow regions. The maximum apparent relative velocity at $z = 75.7$ mm is 50 mm/s for glass particles and < 30 mm/s at $z = 20$ mm. In the near-axis region below the impeller, the apparent relative velocities of the glass particles are around 40 mm/s and are larger than those of the Diakon particles by a factor of 2.5. Above the impeller, only the glass particles show an apparent slip of around 15–30 mm/s. Comparison of the wall jet results below

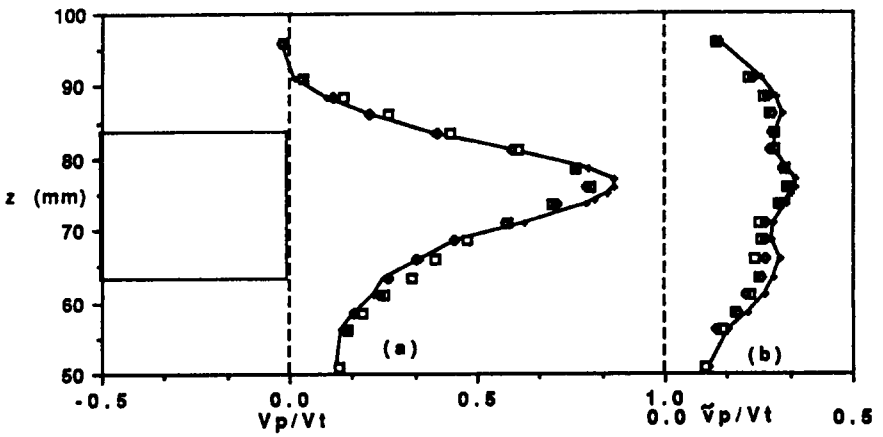

Figure 4. Particle radial velocities in the impeller stream for $D = T/2$, $C = T/4$, $N = 150$ rpm and $\theta = 0°$: (a) mean; (b) r.m.s. Symbols as in figure 2.

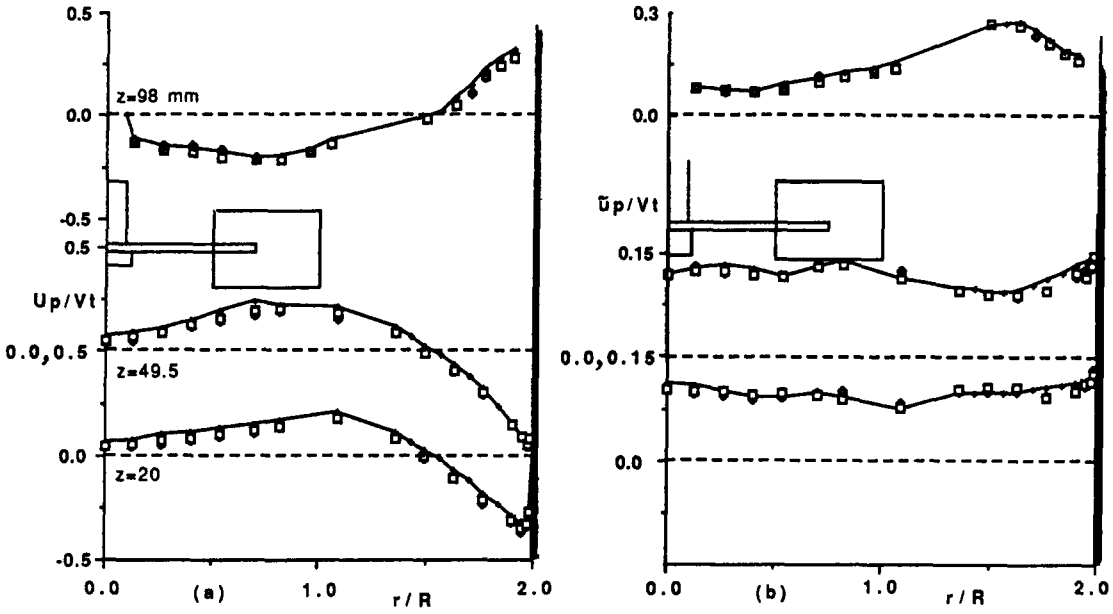

Figure 5. Particle axial velocities above and below the impeller for $D = T/2$, $C = T/4$, $N = 150$ rpm and $\theta = 0°$. (a) mean; (b) r.m.s. Symbols as in figure 2.

the impeller at $z = 75.5$ and 20 mm (downflow) shows that the particles lead at the former location and lag at the latter. The initial lag can be attributed to particle inertia in that region where the particles meet the wall and change direction. Subsequently, the particles accelerate due to gravity and eventually lead the fluid. Above the impeller in the wall jet at $z = 120.3$ mm (upflow) the results show a larger lag than that at $z = 75.7$ mm, since at this axial location the gravity and inertia effects act in the same direction. The particle turbulence levels in the bulk of the flow are similar to those of single-phase flow with a reduction of about 4% in the two-phase flow case. A greater reduction exists in the wall jet regions with levels lower by 7 and 15% Diakon and glass particles; again, as in the impeller stream, the particle turbulence levels of the heavier particles are less than those of the lighter ones by a factor 2.

Figures 4 and 5 present particle mean and r.m.s. velocities for the fourth and fifth flows in table 3, with the larger impeller and smaller clearance, and show similar features to those described above. The radial jet at the impeller tip, figure 4(a), shows that the largest differences between single-phase and the solid-phase profiles are again near the plane of the impeller disc where the apparent relative velocity is about 80 mm/s of $0.072V_t$ for both the 232 and 376.5 μm dia glass particles. These apparent relative velocities are smaller, by about 45%, than those of figure 4 for the same particles due probably to the less steep velocity gradients.

The axial particles mean velocities of figure 5(a) show that the particles lag or lead the fluid in the upflow and downflow situations, respectively, and that the apparent relative velocity changes sign in the near-axis and near-wall regions. Again below the impeller, the particles initially lag ($z = 49.5$ mm) and subsequently lead ($z = 20$ mm) the fluid in the wall jet region. The turbulence results of figures 4(b) and 5(b) show that the intensity of the particle fluctuations is smaller, by up to 23%, than that of the single-phase flow in the impeller stream, and similar for both particle sizes.

The mean velocity of the liquid phase in the presence of the particles is expected to be similar to that of the single-phase velocities at the low volumetric concentration (0.02%), which is well below that (0.3%) suggested by Lumley (1978) for particle-to-particle interaction, and the apparent relative velocities presented above can be considered to be the true values. Equations [3] and [4] underestimate the relative velocity, as in the experiments of Lee & Durst (1982), Tsuji *et al.* (1984) and Nouri *et al.* (1987), because other local effects may contribute to the differences, including the effects of particle inertia (especially where the particles are deflected by solid boundaries or particle collision in the cross-flows), of the Magnus force where the particles are subject to strong velocity gradients and of the migration of particles which depends on the density rate of the carrying fluid to the suspended particles and on the flow direction (Cox & Mason 1971).

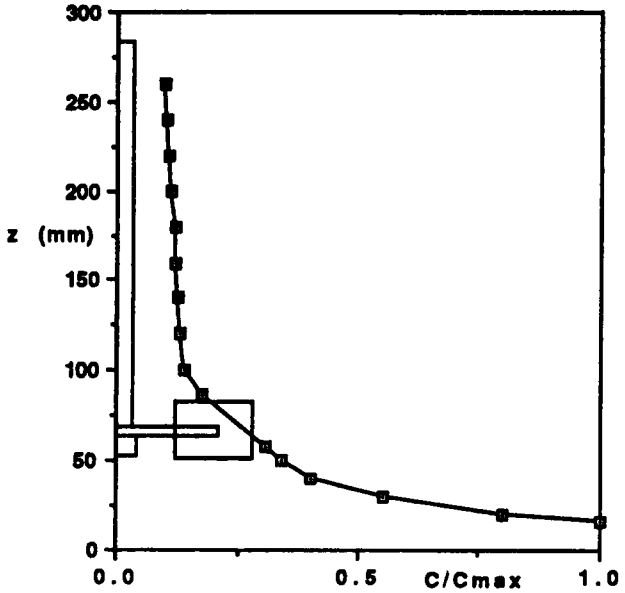

Figure 6. Variation of relative particle concentration along the height of the vessel at $r = 20$ mm, $d_p = 665\ \mu$m, $C_v = 0.5\%$, and for $D = T/3$, $C = T/4$, $N = 3/3$ rpm.

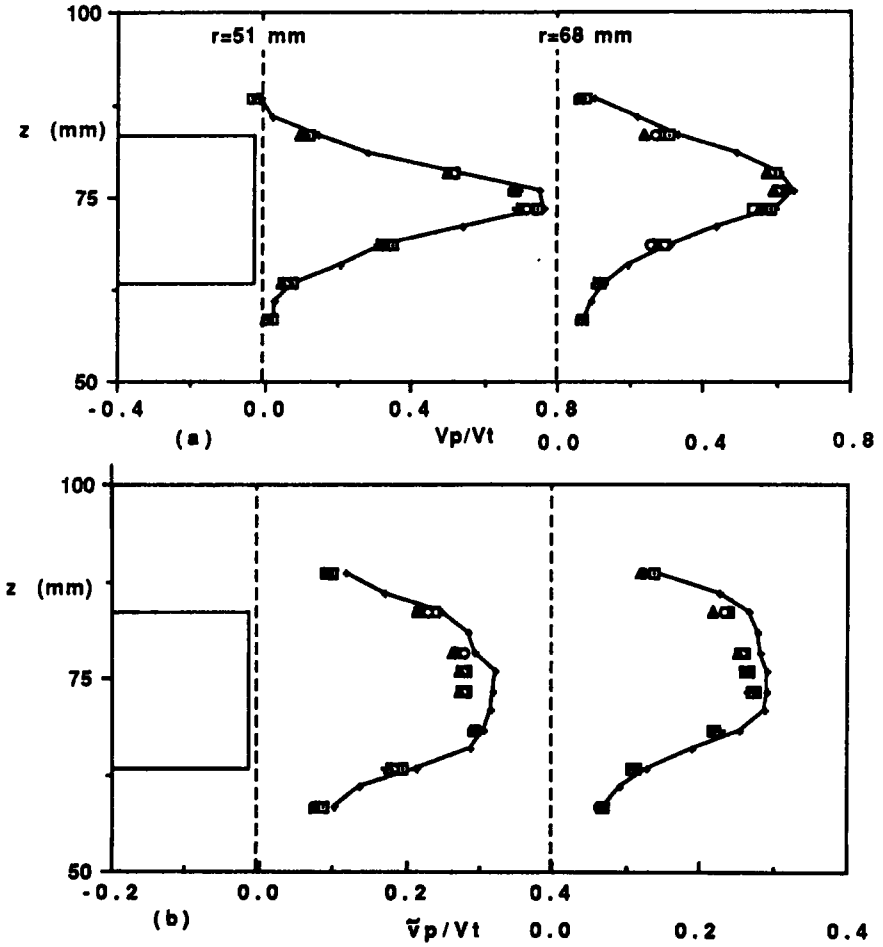

Figure 7. Particle radial velocities as a function of particle concentration in the impeller stream for $D = T/3$, $C = T/4$, $N = 3/3$ rpm and $\theta = 0°$: (a) mean; (b) r.m.s. ———, Single phase; +, $C_v = 0.25\%$; □, $C_v = 0.5\%$; ⊡, $C_v = 0.75\%$; ○, $C_v = 1.75\%$; △, $C_v = 2.5\%$.

3.2. *Particle motion in a moderately dense suspension*

Detailed measurements of the three components of the particle mean and r.m.s. velocity were made for Diakon particles of 665 μm mean dia for different particle volumetric concentrations in a mixture of turpentine and tetraline so that the refractive index of the fluid was the same as that of Diakon particles at 28.5°C. The maximum particle concentration at which velocity measurements could be made was 2.5% in the mixture flow, i.e. 125 times that of the water flow in the previous subsection.

The particle concentration along the height of the vessel was quantified by measuring the number of gas-inclusions inside the particles crossing the measuring control volume per second. The results were obtained for an average particle volumetric concentration of 0.5% and at a fixed radial location, $r = 20$ mm. The maximum measured value was 1.58×10^8 No. of particles/m^3 at $z = 16$ mm which corresponds to a local volumetric concentration of 2.5%; i.e. five times the average value. The distribution of the relative particle concentration is presented in figure 6, and shows a particularly steep gradient below the impeller and a small gradient above it. The local particle volumetric concentration changes from 5 C_v near the bottom of the vessel to 0.5 C_v close to the free surface; i.e. a change of an order of magnitude. The particle concentration gradients along the radius were not measured because variations in the depth of the field would have introduced errors of unknown magnitude.

Particle mean and r.m.s. velocities are presented in figures 7–9 together with the single-phase flow profiles which are shown as solid lines. Figure 7 confirms that the mean radial particle velocity in the impeller stream lags behind the fluid everywhere and that the lag is again more pronounced near the plane of the impeller disc. Further downstream in the jet, this lag is smaller but more uniform along the width of the impeller at $r = 68$ mm than that at $r = 51$ mm. The apparent relative velocity, V_s, increases with particle concentrations so that at the tip of the impeller, $r = 51$ mm,

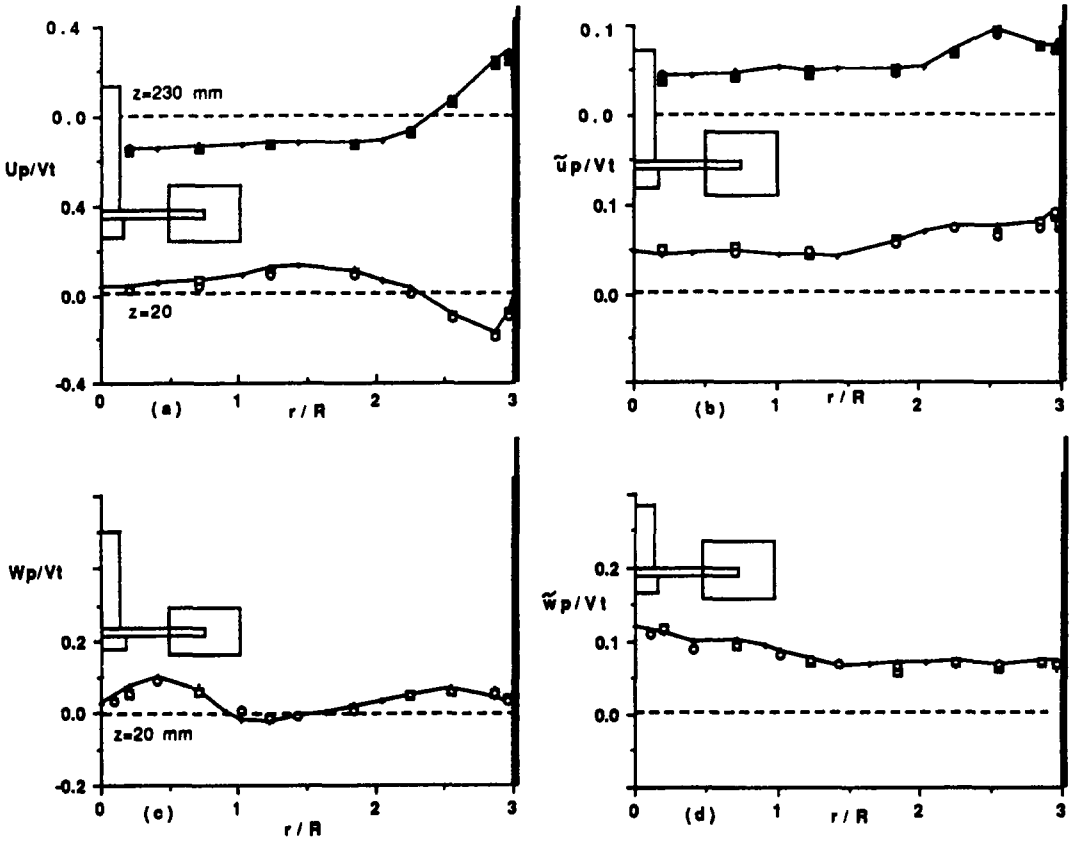

Figure 8. Particle axial velocities as a function of particle concentration above and below the impeller for $D = T/3$, $C = T/4$, $N = 313$ rpm and $\theta = 0°$; (a) axial mean; (b) axial r.m.s.; (c) tangential mean; (d) tangential r.m.s. Symbols as in figure 7.

it increases from 20–100 to 50–120 mm/s for a change in concentration from 0.25 to 2.5%, respectively. This result is consistent with the well-established empirical relationship that the relative velocity is proportional to $(1 - C_v)^{1.325}$ and also in agreement with previous experimental investigations (e.g. Birchenough & Mason 1976; Tsuji *et al.* 1984; Nouri *et al.* 1987; Hardalupas *et al.* 1988; Liu *et al.* 1990). The particle r.m.s. velocities are smaller than those in the single-phase flow by about 15% at the impeller tip and 12% at $r = 68$ mm, and there is no change with concentration. This may be due, in part, to the suppression effect discussed by Hetsroni (1989).

In the bulk of the flow, the particles again lead the single-phase flow in the axial direction, figure 8(a), when the flow is directed downwards and lag when the flow is upwards so that the width of the wall jet is increased below the impeller and decreased above it. The particle velocity decreases slightly everywhere with increasing particle concentration and, as a result, the apparent axial relative velocity decreases in downflow and increases in upflow. The variation of particle velocity with particle concentration in the tangential direction is very small at $z = 20$ mm, figure 8(c), except in the counter-rotating flow region where the width of this region is reduced from 35 mm in the single-phase flow to 22 mm for the solid-phase with smaller negative velocities, suggesting that the adverse pressure gradient is less strong in the presence of the particles.

Figure 9 shows the particle velocities at different axial locations with the maximum measured particle concentration. The axial particle velocities of figure 9(a) show that the apparent relative velocities are smaller in the downflow regions due to the increase in concentration and that, as before, the particles initially lag the fluid in the wall jet below the impeller after the impingement at $z = 58.5$ mm and eventually lead at $z = 20$ mm for the same reason. In the tangential direction, the particles velocities are similar to those of the single-phase flow except in the counter-rotating flow region below the impeller where the particles reduce the width of that region at all axial locations. The particle axial and tangential r.m.s. velocities in the bulk of the flow are similar to those of the single-phase flow except in the wall region where the particles r.m.s. velocities are smaller by about 10% and that there is no change with concentration.

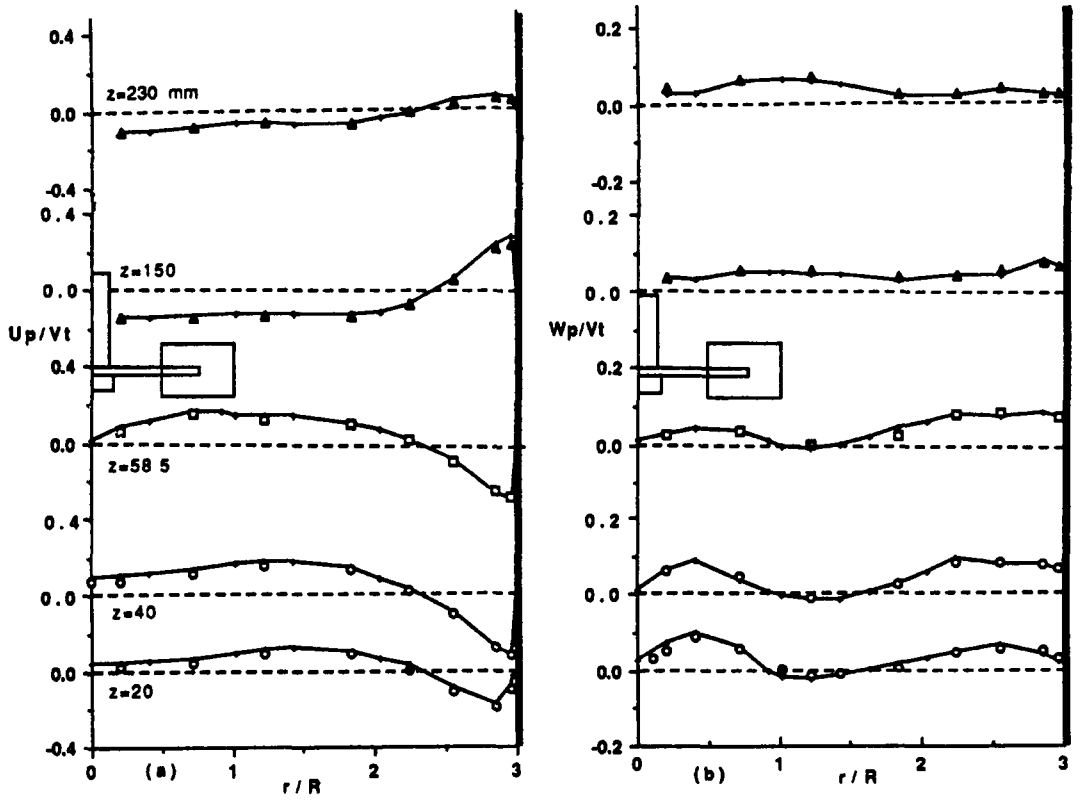

Figure 9. Particle axial velocities above and below the impeller for $D = T/3$, $C = T/4$, $N = 313$ rpm and $\theta = 0°$: (a) axial mean; (b) tangential mean. Symbols as in figure 7.

The results presented in figures 7–9 suggest that the axial and radial particle mean velocities decrease with increasing particle concentration everywhere in the vessel and this is in agreement with all investigations of two-phase flows cited in section 1. The results also show that the particles lag the fluid in the impeller stream, especially around the peak of the jet stream and in the wall jets where the jet stream meets the wall of the vessel, due to particle inertia. Similar results were reported by Nouri *et al.* (1984, 1987) for annular jets around a disc baffles in horizontal and vertical pipes and by Khezzar (1987) in an unsteady flow behind a projectile in a gun barrel.

In turbulent flow, the motion of particles is affected by their inertia, crossing-trajectory and the turbulent flow field. The effect of inertia is to decrease the r.m.s. of the velocities of the particles which depend on the ratio of particle time response to that of the fluid time response (Lumley 1978; Wells & Stock 1983): as demonstrated in section 2, the effect of particle inertia is expected to be small. Where the flow is deflected from solid boundaries, as in the impeller stream and the wall jet, inertia is more important and it is in those regions where there is suppression of r.m.s. velocities. The effect of crossing trajectories is also negligible as the particles free-fall velocities or relative velocities are smaller than those of the single-phase r.m.s. velocities (Wells & Stock 1983).

4. CONCLUDING REMARKS

Measurements of particle mean velocities and the corresponding fluctuation velocities have been obtained in a fully baffled stirred vessel, driven by six-blade impellers with a particle volumetric concentration of 0.02% and up to 2.5% in water and a mixture of turpentine and tetraline, respectively. Refractive index matching allowed velocity measurement in the moderately dense suspension of 2.5% concentration but higher values were prevented by gas-inclusions in the particles. The trends were similar for both water and mixture flows with a particle concentration gradient existing along the height of the vessel so that the local volumetric concentration at $C_v = 0.5\%$ was about $5\,C_v$ in the vicinity of the bottom of the vessel and reduced to $0.5\,C_v$ close to the free surface.

In the impeller stream, the particles lagged the single-phase flow by an amount which was more pronounced near the plane of the impeller disc, with a maximum value of $0.075\,V_t$ for the 2.5% Diakon particles. In general, the particles led the fluid in downflow and lagged in upflow regions. The particle turbulence levels were lower in the impeller stream than those of the single-phase values by about 13 and 25% for Diakon and glass particles in water flow ($C_v = 0.02\%$), respectively, and 15% for Diakon particles in mixture flow ($C_v = 2.5\%$). In the bulk of the flow, the turbulence levels of the particles and fluid were similar except in the wall jet where the particles levels were lower by up to 10%.

Within the measured range, the apparent relative velocities of the glass particles were larger than those of the Diakon particles by factors of 2 and 2.5 in the impeller stream and in the bulk of the flow, respectively, and the particle fluctuating velocities of the heavier particles were lower than those of lighter particles. The axial and radial particle mean velocities decreased with increasing particle concentration by up to 5 and 10% in the impeller stream and in the bulk of the flow, respectively, for a change of C_v from 0.25 to 2.5%: the particle turbulence results were unaffected. The effect of particle size, within measured size range, on particle mean and r.m.s. velocities was small.

Acknowledgements—Financial support from the European Economic Community, Unilever Research plc and ICI plc under a Brite contract is gratefully acknowledged.

REFERENCES

BACHALO, W. D. & HOUSER, M. J. 1984 Phase/Doppler spray for simultaneous measurements of drop size and velocity distribution. *Opt. Engng* **23**, 583–590.

BIRCHENOUGH, A. & MASON, J. S. 1976 Local particle velocity measurements with a laser anemometer in an upward flowing gas–solid suspension. *Powder Technol.* **14**, 139–152.

COX, R. G. & MASON, S. G. 1971 Suspended particles in fluid flow through tubes. *A. Rev. Fluid Mech.* **3**, 291–316.

DURST, F. 1982 Review-combined measurements of particle velocities, size distributions, and concentrations. *Trans. ASME* **104,** 284–296.

DURST, F. & ZARE, M. 1975 Laser Doppler measurements in two-phase flows. In *Proc. LDA Symp.*, Univ. of Denmark, Copenhagen, pp. 403–429.

EINAV, S. & LEE, S. L. 1974 Particles migration in laminar boundary layer flow. *Int. J. Multiphase Flow* **1,** 73–88.

HARDALUPAS, Y. 1986 Phase-Doppler anemometry for simultaneous particle size and velocity measurements. Fluids Section Report FS/86/14, Mech. Engng Dept, Imperial College, London.

HARDALUPAS, Y., TAYLOR, A. M. K. P. & WHITELAW, J. H. 1989 Velocity and particle-flux characteristics of turbulent particle-laden jets. *Proc. R. Soc. Lond.* **A426,** 31–78.

HETSRONI, G. 1989 Particles–turbulence interaction. *Int. J. Multiphase Flow* **15,** 735–746.

KHEZZAR, L. 1987 Experiments with steady and unsteady confined turbulent flows. Ph.D. Thesis, Univ. of London, Imperial College.

LEE, S. L. & DURST, F. 1982 On the motion of particles in turbulent flows. *Int. J. Multiphase Flow* **8,** 125–146.

LIU, C. H., NOURI, J. M., WHITELAW, J. H. & TSE, D. G. N. 1990 Particle velocity in swirling, confined flow. *Combust. Sci. Technol.* **68,** 131–145.

LUMLEY, J. L. 1978 *Two-phase and Non-Newtonian Flows in Turbulence* (Edited by BRADSHAW, P.). *Springer Topics in Applied Physics* **12,** 289–324.

MODARRESS, D., WUERER, J. & ELGOBASHI, S. 1982 An experimental study of a turbulent round two-phase jet. AIAA Paper 82-0964.

MODARRESS, D., TAN, H. & ELGOBASHI, S. 1983 Two-component LDA measurement in a two-phase turbulent jet. AIAA Paper 83-0052.

NOURI, J. M. 1988 Single and two phase flows in ducts and stirred reactors. Ph.D. Thesis, Imperial College, Univ. of London.

NOURI, J. M. & WHITELAW, J. H. 1990 Effects of size and confinement on the flow characteristics in stirred reactors. Presented at the *5th Int. Symp. on Applications of Laser Techniques to Fluid Mechanics.*

NOURI, J. M., WHITELAW, J. H. & YIANNESKIS, M. 1984 The flow of dilute suspension of particles around axisymmetric baffles. Fluids Section Report FS/84/18, Mech. Engng Dept, Imperial College, London.

NOURI, J. M., WHITELAW, J. H. & YIANNESKIS, M. 1987 Particle motion and turbulence in dense two-phase flow. *Int. J. Multiphase Flow* **13,** 729–739.

NOURI, J. M., WHITELAW, J. H. & YIANNESKIS, M. 1988 A refractive index matching technique for solid/liquid flows. *Laser Anemom. Fluid Mech.* **3,** 335.

OLDSHUE, J. Y. 1983 *Fluid Mixing Technology*, McGraw-Hill, New York.

SAFFMAN, M., BUCHHAVE, P. & TANGER, H. 1986 Simultaneous measurements of size, concentration and velocity of spherical particles by laser Doppler method. *Laser Anemom. Fluid Mech.* **2,** 85–103.

SOO, S. L. 1967 *Fluid Dynamics of Multiphase Systems.* Blaisdell, Waltham, MA.

TSUJI, Y. & MORIKAWA, Y. 1982 LDA measurements of an air–solid two-phase flow in a horizontal pipe. *J. Fluid Mech.* **120,** 385–409.

TSUJI, Y., MORIKAWA, Y. & SHIOMI, H. 1984 LDA measurements of an air–solid two-phase flow in a vertical pipe. *J. Fluid Mech.* **139,** 417–434.

UHL, V. W. & GRAY, J. B. 1986 *Mixing: Theory and Application*, Vol. 1. Academic Press, New York.

WELLS, M. R. & STOCK, D. E. 1983 The effects of crossing trajectories on the dispersion of the particles in turbulent flow. *J. Fluid Mech.* **136,** 31–62.

YIANNESKIS, M., POPIOLEK, Z. & WHITELAW, J. H. 1987 An experimental study of the steady and unsteady flow characteristics of stirred reactors. *J. Fluid Mech.* **175,** 537–555.